Modeling of the deposition of Na Clusters on MgO(001)

M. Bär,[1] P. M. Dinh,[2,3] L. V. Moskaleva,[4] P.-G. Reinhard,[1] N. Rösch,[4] and E. Suraud[2,3]
[1]*Institut für Theoretische Physik, Universität Erlangen, Staudtstrasse 7, 91058 Erlangen, Germany*
[2]*Laboratoire de Physique Théorique (IRSAMC), Université de Toulouse–UPS, F-31062 Toulouse, France*
[3]*LPT (IRSAMC), CNRS, F-31062 Toulouse, France*
[4]*Department Chemie and Catalysis Research Center, Technische Universität München, 85747 Garching, Germany*
(Received 24 January 2009; revised manuscript received 12 October 2009; published 4 November 2009)

We investigate the dynamics of deposition of small Na clusters on MgO(001) surface. A hierarchical modeling is used combining quantum mechanical with molecular mechanical description. Full time-dependent density-functional theory is used for the cluster electrons while the substrate atoms are treated at a classical level. We consider Na_6 and Na_8 at various impact energies. We analyze the dependence on cluster geometry, trends with impact energy, and energy balance. We compare the results with deposit on the much softer Ar(001) surface.

DOI: 10.1103/PhysRevB.80.195404 PACS number(s): 34.50.Lf, 36.40.Sx, 68.47.Jn

I. INTRODUCTION

A major branch of present-days cluster research comprises clusters in contact with solid surfaces, for an overview see, e.g.,[1–4] The interaction of these two entities gives rise to a rich scenery of effects such as, e.g., chemical reactions at surfaces,[5–7] particularly, catalytic applications,[8–10] or modified optical response.[11–13] One crucial aspect here is the process of cluster deposition, which is relevant for synthesis and for analysis of clusters in contact with surfaces. Moreover, the deposition dynamics as such is an interesting and demanding process due to the subtle interplay of the impact of interface energy, electronic band structure of the substrate, and surface corrugation. Accordingly, there is a wealth of investigations on cluster deposition, experimentally oriented,[14–21] theoretically with molecular dynamics (MD) techniques[22–26] or more detailed quantum mechanical methods,[27–33] for reviews see.[2,8,34] Although addressing the same physical processes, these various theoretical approaches, relying on different approximations, often provide useful complementary information. Recently, we have investigated deposition dynamics of Na clusters on Ar(001) surface.[33,35,36] The aim of this paper is to continue these theoretical studies now considering deposition dynamics of Na clusters on a much "harder" surface than Ar, namely, MgO(001) insulator surfaces. The structural properties and optical response of Na_n on MgO have already been studied in great detail in using the present computational approach.[37] Both Ar and MgO are similar in that they are both insulators with a large band gap, but they differ significantly in other important properties. There are, however, large differences in other properties. Ar is a Van-der-Waals bound material, thus very soft with little surface corrugation. On the other hand, MgO is an ionic crystal, well bound and with large surface corrugation. It is, thus, most interesting to see how deposition dynamics proceeds in that case, as such, and at variance with the Ar case.

The theoretical description of clusters on surfaces is very involved due to the huge number of degrees-of-freedom of these systems. This holds the more so for dynamics. The vast majority of theoretical studies thus resorts to MD simulations using effective force fields between the atoms, as mentioned above.[22–26,34] These are comparatively inexpensive and can provide a pertinent picture of the leading atomic transport processes. Metal clusters are more than an ensemble of atoms because they held together by delocalized bonds (due to a common electron cloud); in consequence, they show pronounced shell effects.[38–40] This makes a quantum mechanical description of cluster dynamics advisable. Most of the fully quantum mechanical pictures make compromises in concluding on dynamical features from a series of static calculations. A true Born-Oppenheimer MD for deposition of Pd clusters on MgO substrate can be found in.[29] The enormous expense of such high-level calculations limits the size of the systems, particularly the size of the representative for the substrate. On the other hand, there are many situations, in which the substrate is much more inert than the cluster. Our test case of Na clusters on MgO(001) belongs to that class. This suggests to use a hierarchical description where the cluster electrons are treated quantum mechanically by full time-dependent density-functional theory (TDDFT) while the substrate atoms are handled at a lower level of refinement by classical motion. This modeling belongs to the family of coupled quantum-mechanical with molecular-mechanical methods (QM/MM) which are often used in other fields as, e.g., biochemistry[41–43] or surface physics.[44,45] In earlier studies, we developed and applied a QM/MM model for Na clusters in contact with Ar.[35,36,46–48] We have shown that it was most crucial to include properly the dynamical polarizability of the substrate when exploring truly dynamical processes as we aim at. Recently, we extended the modeling to Na clusters on MgO surfaces, again including dynamical polarizability.[37] Here we take up that model and apply it to a study of deposition dynamics. We will consider Na_6 and Na_8 as test cases. These two clusters have very different geometries and binding properties which allows to explore qualitatively the impact of cluster properties on the deposition process.

The paper is organized as follows: In Sec. II, we summarize the QM/MM model for Na clusters on MgO. Section III presents results tracking the detailed dynamics in terms of trajectories and analyzing the processes with respect to en-

TABLE I. The dynamical degrees-of-freedom of the model. Upper block : Na cluster. Lower block : Active cell of the MgO substrate. See text for details.

$\varphi_n(\vec{r}),\ n=1,\ldots N_{\mathrm{el}}$	Valence electrons of the Na cluster
$\vec{R}_{i^{(\mathrm{Na})}},\ i^{(\mathrm{Na})}=1\ldots N_{\mathrm{i}}$	Positions of the Na^+ ions
$\vec{R}_{i^{(c)}},\ i^{(c)}=1\ldots M$	Positions of the O cores
$\vec{R}_{i^{(v)}},\ i^{(v)}=1\ldots M$	Center of the O valence cloud
$\vec{R}_{i^{(k)}},\ i^{(k)}=1\ldots M$	Positions of the Mg^{2+} cations

ergy transfer and energy balance. Conclusions are summarized in Sec. IV.

II. BRIEF SUMMARY OF THE MODEL

A. Degrees-of-freedom

The hierarchical QM/MM model has been detailed in.[37] We review that here briefly. The various constituents and their degrees-of-freedom are summarized in Table I. The Na cluster is treated in standard fashion.[49,50] Valence electrons are described in terms of single-particle wave functions $\varphi_n(\vec{r})$ and the complementing Na^+ ions are handled as charged classical point particles characterized by their positions $\mathbf{R}_{i^{(\mathrm{Na})}}$, see upper block of Table I. The electrons are described by TDDFT at the level of the local-density approximation (LDA) The substrate is composed of two species: Mg^{2+} cations and O^{2-} anions. The cations are electrically inert and can be treated as charged point particles; they are labeled by $i^{(k)}$. The anions are easily polarizable, an aspect which is described by allowing for two constituents: a valence electron distribution (labeled by $i^{(v)}$) and the complementing core (labeled by $i^{(c)}$). Each of these three types of constituents is described as a classical degree-of-freedom in terms of positions $\vec{R}_{i^{(\mathrm{type})}}$, see the lower block of Table I. The difference $\mathbf{R}^{(c)}-\mathbf{R}^{(v)}$ represents the electrical dipole moment of the O^{2-} anion and is thus allowed, by construction, to explicitly evolve in time, as a function of the local electric field due to all constituents of the system at a given instant.

The combined system is sorted in four stages of decreasing activity, as sketched in Fig. 1. The Na cluster is treated at the highest level of theory with full TDLDA-MD. The Mg and O ions of the substrate are arranged in fcc crystalline order corresponding to bulk MgO, with a lattice parameter of 7.94 a_0. All dynamical degrees-of-freedom for Mg and O, as listed in Table I, are taken into account in an active cell of the MgO(001) surface region underneath the Na cluster, denoted "zone I" in the sketch. The active cell is continued by an outer region of MgO material (zone IIa) where the ionic centers of Mg and O are kept fixed, while oxygen dipoles still remain active degrees-of-freedom. Thus, zone I together with zone IIa constitute the "active cell." Anything farther out ("zone IIb") is totally frozen at crystalline configuration and only its Madelung potential is considered. The effect of the outer region on the active part is given by a time-independent shell-model potential;[51] the actual parameters of this force field were adopted from.[45]

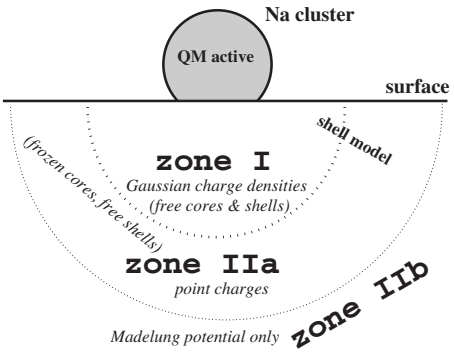

FIG. 1. Schematic view of the hierarchical model for Na_N on MgO(001) surface.

The active cell consists of three layers, each containing square arrangements of 242 Mg^{2+} cations and 242 O^{2-} anions. The ions in the lowest layer are fixed at the bulk structure to prevent them from relaxing and forming an artificial second surface. The volume where ions and electrons are mobile (zone I) has a diameter of 24 a_0, all layers together (zone I+IIa) extend to 42 a_0 from the surface. Bulk structure farther out is modeled by the Madelung potential. Checks with models of a larger number of layers showed that three layers provide an adequate description of the very inert MgO material. [The soft Ar(001) substrate, used for comparison later on, is more critical and requires at least four active layers plus two frozen ones.]

B. Energy

The total energy is composed as $E=E_{\mathrm{Na}}+E_{\mathrm{MgO}}+E_{\mathrm{coupl}}$ where E_{Na} describes an isolated Na cluster, E_{MgO} the MgO(001) substrate, and E_{coupl} the coupling between the two subsystems. For E_{Na}, we take the standard TDLDA-MD functional as in previous studies of free clusters[49,50] including an average self-interaction correction.[52] The energy of the substrate and the coupling to the Na cluster consist of long-range Coulomb energy and some short-range repulsion, which is modeled through effective local core potentials.[45] To avoid the Coulomb singularity and to simulate the finite extension of Mg^{2+} and O^{2-} ions, we associate a smooth charge distribution $\rho(\vec{r})\propto\exp(-\vec{r}^2/\sigma^2)$ with each of these ionic centers. We associate a similar smooth charge distribution to the O^{2-} valence cloud as well. This altogether yields a soft Coulomb potential to be used for all active particles.

C. Calibration of the QM/MM model

The calibration of the whole model has to address three issues: the cluster as such, the environment as such, and the coupling between both. The modeling for the cluster is taken over from work on free clusters.[49,50] The model parameters for the pure environment are the same as in previous studies of MgO(001).[45,53] The parameters for the coupling between environment and Na cluster were calibrated from scratch. The tuning for Na@MgO(001) was performed using fully quantum-mechanically computed Born-Oppenheimer surfaces for Na atoms and Na^+ ions on MgO(001) from.[53] These surfaces were computed at four different substrate sites (O^{2-},

Mg^{2+}, hollow, bridge) down to close distances where the full substrate repulsion was felt. For further details and the actual model parameters, see Ref. 37.

Two quantitative points are worth to be mentioned. The modeling achieves a barrier for penetration of cluster electrons into the substrate, which reproduces nicely the large band gap of 6.9 eV for MgO. The fully quantum mechanical calculations show that electron transfer from the substrates O^{2-} anions to a Na atom remains below 0.1 charge units down to the closest distances considered (where the repulsive energy comes about the band gap). Transfer from the Na atom to the Mg^{2+} cation is totally ignorable. This nice decoupling of ad-atoms and substrate is probably a feature of simple metals. Noble metals, e.g., can develop a more involved surface chemistry due to the closeness of the *d* shell.[29]

D. Solution scheme

From the energy functional, once established, one derives the static and dynamical equations variationally in a standard manner. The numerical solution of the coupled quantum-classical system proceeds as described in.[37,54,55] The electronic wave functions and spatial fields are represented on a Cartesian grid in three-dimensional coordinate space. The numerical box employed here has a size of $(64\ a_0)^3$. The spatial derivatives are evaluated via fast Fourier transform. The ground-state configurations were found by interlaced accelerated gradient iterations for the electronic wave functions[56] and simulated annealing for the ions in the cluster and the substrate. Propagation is done by the time-splitting method for the electronic wavefunctions[57] and by the velocity Verlet algorithm for the classical coordinates of Na^+ ions and MgO constituents.

All the collisional processes studied in the current paper proceed on an ionic time scale, i.e. slow as compared to electronic motion. True electronic excitations are thus extremely small. For example, ionization stays safely below a fraction of 0.001 electrons. It would then be well justified to use Born-Oppenheimer-MD rather than full TDLDA-MD, as long as one carefully maintains the crucial dipole polarizability of the substrate. But the TDLDA-MD scheme is so efficient that it is still preferable for reasons of computing time. Remind that the dipole response of the substrate needs to be propagated at electronic time scale and dipole stepping is more economic than fully relaxing the dipoles in each Born-Oppenheimer step.

E. Preparation of the system

First, the ground state structures of the pure MgO surface and of the free-Na cluster are determined for the given model by simulated annealing. The Na cluster is then placed at a certain distance from the surface of the substrate. A distance of about 15 a_0 has turned out to be sufficient. After that a Galilean transformation is applied to the cluster. This means that each of the cluster ions is given a momentum $\vec{P}_0$ in the direction toward the surface and the electronic wave functions are boosted by an equivalent momentum as

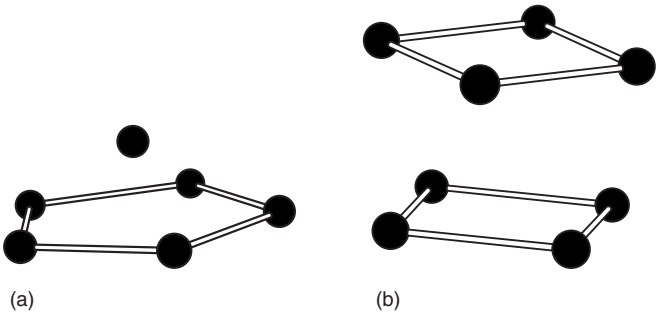

FIG. 2. The structures of free Na_6 (left) and Na_8 (right). The bond distance along the five-fold ring of Na_6 is 6.5 a_0 and the top ion resides 3.1 a_0 above the ring. The bond distance in the two four-fold rings of Na_8 is 6.2 a_0 and the distance between the two rings is 5.8 a_0.

$$\varphi_i(\vec{r}) \rightarrow \exp(\imath \vec{p}_0 \cdot \vec{r})\varphi_i(\vec{r}), \tag{1}$$

where $\vec{p}_0 = \frac{m_e}{M}\vec{P}_0$, m_e and M are the electron and Na ion mass, respectively. This provides the initial state from which on the system propagates in a straightforward manner according to the TDLDA-MD equations.

F. Structure of the test cases

The starting point of deposition dynamics are well-relaxed structures for the clusters and pure MgO(001) surface. These had been discussed extensively in.[37] The MgO surface is a cut through cubic crystal structure. From the top, one sees a chess-board structure with alternating Mg and O ions. For the Na clusters, we will use here Na_6 and Na_8 as examples. The initial state starts from free clusters. Their structures are shown in Fig. 2. Note that the vertical axis in the figure will represent the direction perpendicular to the surface in the forthcoming deposition processes (z axis). Na_6 is strongly oblate consisting out of a ring of five ions topped by one single ion. Na_8 has a highly symmetric configuration out of two rings of each four ions tilted relative to each other by 45° to minimize Coulomb energy. The electronic cloud of Na_8 is close to spherical shape because $N=8$ electrons correspond to a strong shell closure for Na clusters.[40] It is important to note that the bond distances for Na_8 (6.2 a_0) are not far from the diagonal distance between oxygen sites in the MgO(001) surface (5.7 a_0) while the dimensions of the fivefold ring in Na_6 do not fit well to the surface. That will play a role in the dynamical evolution studied later on. The equilibrium distance of the lower cluster plane (facing toward the surface) and the first surface layer is 5 a_0.

III. RESULTS AND DISCUSSION

A. Na monomer on MgO—the influence of sites

A two component system such as MgO has more possible adsorption sites than a homogeneous material such as an argon substrate. The properties of an oxygen site are much different from those of the magnesium site because of the much larger polarizability of oxygen. We will, thus, consider four positions with respect to the surface : O site, Mg site,

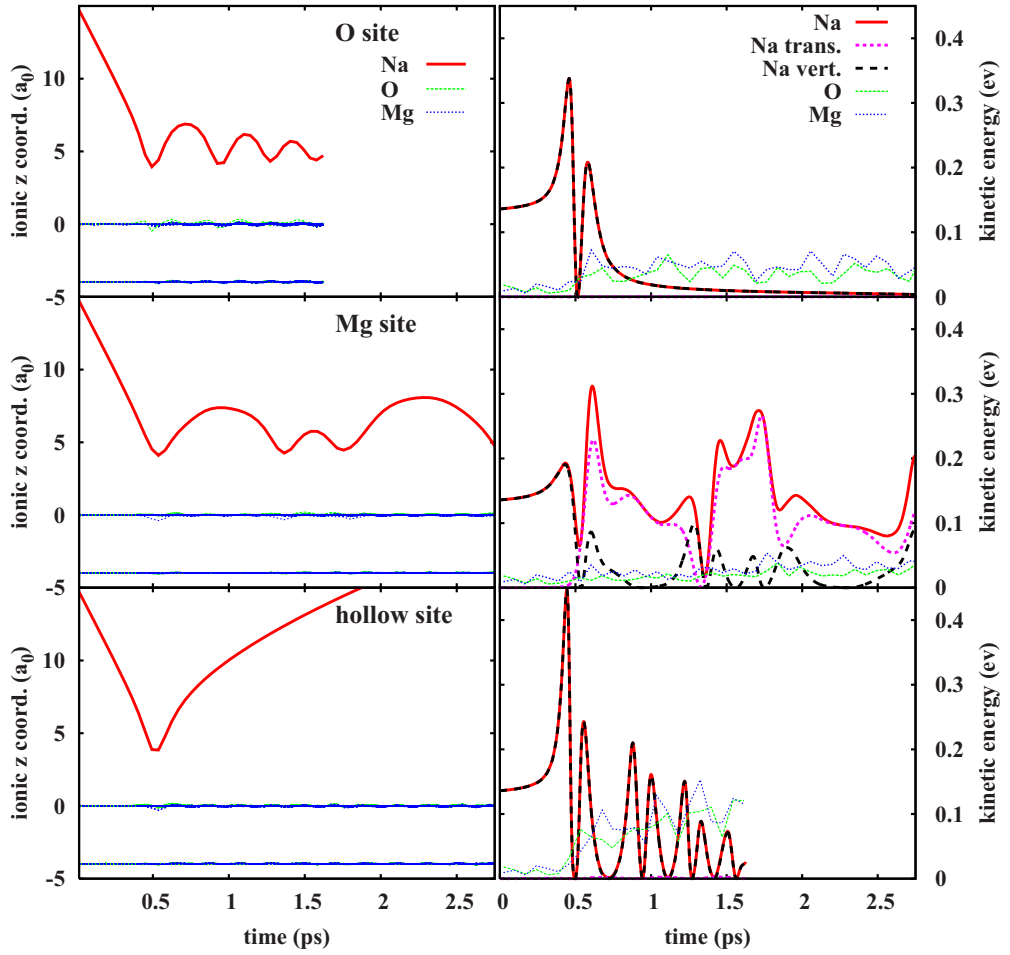

FIG. 3. (Color online) Time evolution of the ionic coordinates and kinetic energies E_{kin} for the deposition of a Na monomer on MgO(001) with initial kinetic energy E_{kin}^{0}=0.136 eV, impinging on various sites : O site (top), Mg site (center) and hollow site (bottom). Left : z coordinates of Na (thick line), Mg (thin curve), and O (gray line) cores. Right : Total E_{kin} of Na (thick gray or red curve), lateral E_{kin} of Na (magenta dots), vertical E_{kin} of Na (black dashes), and total E_{kin} of Mg (thin dark or blue curve) and O (thin light or green curve) cores.

hollow and bridge. The structure calculations of[37] have shown that O, due to its large polarizability, is the most attractive site while Mg acts like a repulsive site on the cluster. This is in agreement with quantum chemical ground state calculations of transition metals on MgO.[53]

In order to check the adsorption properties of the various sites, we first study the deposition dynamics of a Na monomer. We briefly remind the static properties of Na@MgO(001). The O site is most attractive, binding Na 5 a_0 above the surface with energy 0.25 eV. The Mg site is dominantly repulsive. The hollow and bridge sites lie in between these extremes. For deposition dynamics, the atom was initialized 15 a_0 away from the substrate above an O site, Mg site or hollow site respectively, each with an initial momentum along z direction, pointing perpendicular toward the surface with a magnitude corresponding to a kinetic energy E_{kin}^{0}=0.136 eV. Figure 3 shows the results of the simulation. The z coordinates are chosen such that the (average) MgO surface layer resides at z=0. The simplest case is the impact on the O site. The atom approaches the surface up to a distance of 4.5 a_0 which is reached at about 500 fs and transfers part of its momentum to the substrate ions. The transfer proceeds at a very short time scale. The surface itself is excited mainly by the first collision which initially only affects the ions in the immediate vicinity of the atom at closest impact. The perturbation quickly spreads over the surface, but the associated sound wave does not penetrate very deep into the surface. The oscillations in the third layer are already almost negligible. After the instant of closest contact, the atom bounces back, but it has already lost so much energy that it cannot escape from the surface anymore. Thus it performs damped oscillations, with each bounce transferring some momentum to the surface and being practically adsorbed within the first 2 ps. The final distance approaches nicely the equilibrium distance of 5 a_0. The right upper column of Fig. 3 shows the corresponding kinetic energy contributions. In the first 400 fs, the attraction from the MgO substrate leads to a rapid increase in the kinetic energy of the atom up to 0.45 eV. At the point of closest contact, the repulsive part of the interface potential stops the atom abruptly. That first collision transfers by far the largest amount of energy to MgO, whereas at all subsequent collisions the energy decreases more slowly. In order to check that the oscillations proceed only perpendicular to the surface, the kinetic energy of the Na atom has been split into contributions from perpendicular (or vertical) and parallel (or transverse) motion. The

latter is too small to be visible in Fig. 3 and practically negligible. Thus, the motion of Na proceeds strictly perpendicular to the surface. The kinetic energy transferred to the MgO can also be read off from Fig. 3 (see right upper panel). The contributions from oxygen and magnesium are given separately. Oxygen ions are the lighter species and therefore react first being quickly accelerated. About 100 fs later, the energy has already been distributed almost equally over both ion types.

The dynamics behaves totally different if the atom impinges on the (repulsive) Mg site, see middle panels of Fig. 3. At first glance, the z component of the Na trajectory looks quite similar to the case before. But one notes that the motion is not damped after the first reflection. The kinetic energies (middle right panel) give a clue on the process. There is much less energy transfer at first impact which is related to the fact that the Mg^{2+} ion is more inert. And there is a significant amount of lateral kinetic energy for the Na atom creeping up after impact time at 500 fs. In fact, most of the kinetic energy is now in lateral motion. The atom is deflected by the Mg^{2+} ion. It is to be noted that the annealing of the substrate configuration leaves a small amount of symmetry breaking with fluctuations of the atomic positions of about 0.05 a_0. This small symmetry breaking allows the atom to acquire sideward momentum and so it bounces away in sideward direction, hops over the surface several times changing direction whenever it comes close to another surface ion. The motion is almost undamped because little energy is transferred to the surface after the first collision. The atom has thus still too much energy to be caught by a certain site of the surface. But as the atom cannot escape the surface as a whole, it will continue to lose slowly energy and finally be attached to an oxygen site, long after the simulation time of 3 ps.

The bottom panels of Fig. 3 show the case of impact at a hollow site. We see again the immediate reflection at impact time associated with fast energy transfer. Less energy is transferred than on the other sites (see upper and middle panels) and thus the bounce back has a much larger amplitude than in both other cases. The Na motion remains strictly perpendicular to the surface as practically no lateral kinetic energy can be seen. The vertical kinetic energy is almost approaching zero because the departing Na atom has to work against the polarization potential. The case is at the limits of our box size and energy resolution such that we cannot decide whether the atom will finally escape with extremely small kinetic energy, or will bounce back and relax to an adsorption site on a very long time scale. Nevertheless, we find it worth noting that the hollow site seems sufficiently attractive to hinder deflection toward the still more attractive oxygen site.

B. Cluster deposition

1. Case of symmetric Na_8

The analysis of Sec. III A has shown the importance of surface site nature in the deposition process. Depositing an extended object such as a cluster will lead to a mixed situation because the ions of the cluster will necessarily be placed above different sites. In the following, we will discuss deposition of Na_8 and Na_6, which have very different structures and so promise to show different deposition scenarios. As a first step in the analysis, we shall consider detailed ionic trajectories both perpendicular and parallel to the surface. The case of Na_8 is shown in Fig. 4. The cluster was injected with its symmetry axis pointing through a hollow site and with the lower ring facing closer to bridge sites. The top panels show a soft deposition where the initial kinetic energy is 0.109 eV (0.0136 eV per Na ion). The left-upper panel shows that the cluster is slightly accelerated in the initial phase, due to the attraction from the surface. But that acceleration differs for the different ions on the lower ring because they approach different sites on the surface. At the same time, the cluster rotates in the x-y plane to bring the four ions of the lower ring closer to the attractive oxygen sites. One may spot that from the top view in the right-upper panel. At the point of closest impact around 900 fs, the cluster transfers some momentum to the surface. The substrate ions are slightly displaced from their equilibrium positions and oscillate around their new positions. The disturbance quickly decreases from layer to layer. The perturbation is negligible already in the fourth layer. The complicated detailed dynamics of the Na ions indicates that a major part of the translational kinetic energy is converted into heat, i.e., kinetic energy of the motion relative to the center of mass, as will be confirmed in Sec. III D. Nevertheless, the cluster basically keeps its original structure during the whole simulation period of 9 ps. In particular the two rings, each made of four ions, always stay clearly separated from each other. The top-down projection of the trajectories (see right-hand side of Fig. 4) shows that the cluster as a whole (or its center of mass) remains oscillating around the point of impact. The remaining kinetic energy of the cluster does apparently not suffice to overcome the surface corrugation barriers. This is related to the fact that the Na_8 structure fits approximately well to the structure and binding distance of MgO, see Sec. II F.

The middle panels of Fig. 4 show a more robust deposition dynamics with initial kinetic energy $E^0_{\mathrm{kin}}=1.09$ eV. The initial velocity is higher and the impact time comes earlier, now at 450 fs. The pattern remains, in principle, similar to the softer deposition. There is little momentum transfer to the substrate, strong internal excitation of the cluster, and the cluster is not departing too far from the impact point. However, perturbations are much larger, yielding larger amplitudes in vertical and lateral motion. As a consequence, the two rings of Na_8 are now not always clearly separated. Nevertheless, the typical structure of Na_8 reappears from time to time as we will see later. The top-down projection of the trajectories (middle right panel of Fig. 4) indicates a new effect, a sideward drift from one adsorption site to the next equivalent site. This sideward drift is again induced by the interplay between attractive O and repulsive Mg sites. The chaotically moving Na ions explore a strongly corrugated surface which leads to occasional side kicks from the repulsive Mg sites.

The bottom panels of Fig. 4 show a hard collision with initial kinetic energy $E^0_{\mathrm{kin}}=10.9$ eV. Internal cluster and excitation and surface perturbation are, of course, again larger.

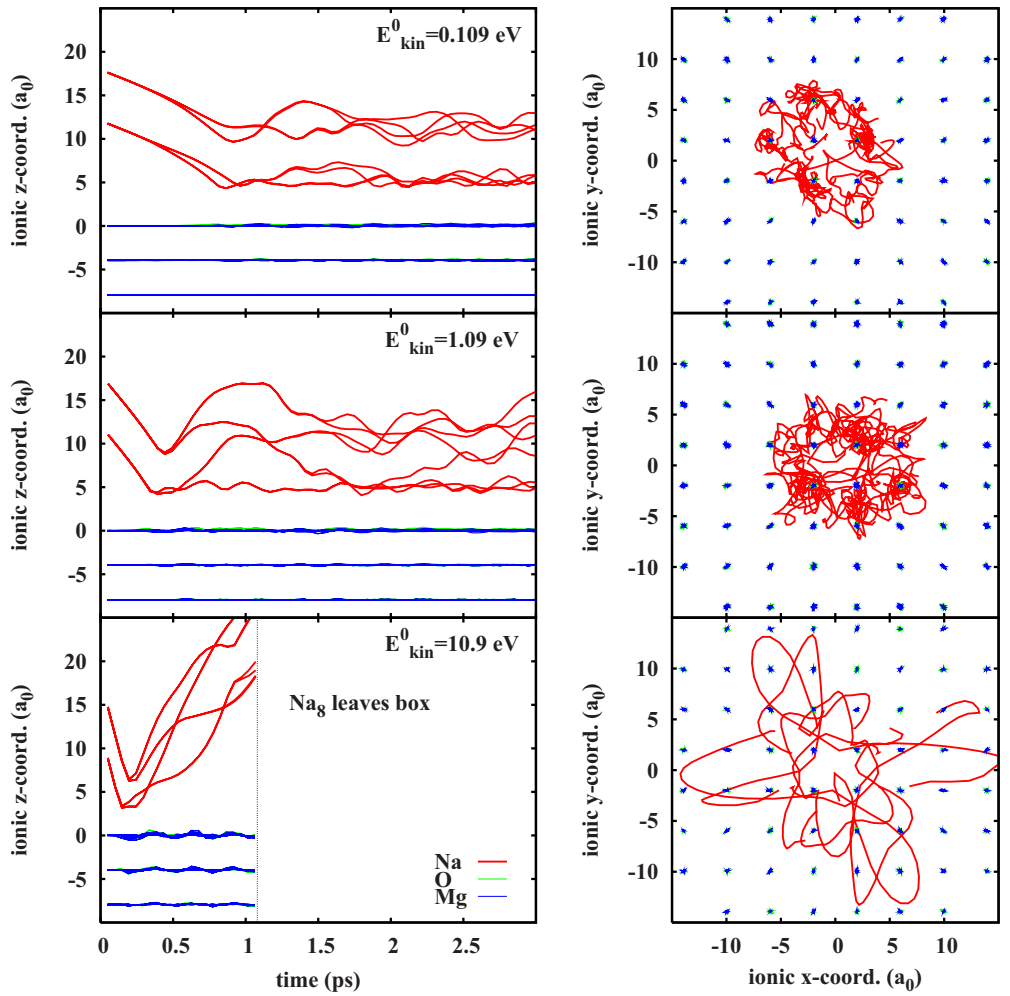

FIG. 4. (Color online) Left : Time evolution of the ionic z-coordinates of Na_8 approaching MgO(001). Right : Projection of the Na and MgO trajectories into the x-y plane; the figures are vertically sorted by increasing initial kinetic energy : Soft deposition (top), robust deposition (center), reflection (bottom).

The new feature is that the cluster is reflected from the surface and leaves the numerical box at about 1 ps, however with huge internal excitation. It is not clear whether the departing cluster will stay asymptotically stable. That is beyond our simulation capacity.

Figure 5 complements the view within showing a sequence of snapshots of the detailed structure for each of the three cases discussed above. The uppermost panel for soft deposition nicely shows the initial rotation of the cluster to match the attractive oxygen sites. The further snapshots indicate the sizeable internal excitation, however remaining small enough to see at all times clearly the two-ring structure of Na_8. The middle panel for more robust deposition also presents the much larger cluster oscillations where the original cluster structure is often blurred, but reappears shortly at other times. That demonstrates the surprisingly good binding of Na clusters, particularly the Na_8 cluster with its magic electron configuration. The lowest panel shows the case of reflection. Obviously, some ions would like to stick to the surface, but are finally caught back by the cluster which departs in a highly excited state.

2. Case of strongly oblate Na_6

Results for the deposition of Na_6 are shown in Fig. 6. The impact energy is varied and all three cases start from the same initial configuration where the top ion of Na_6 (see Sec. II F) is facing away from the substrate and the fivefold ring is parallel to the surface. The general features are similar to the case of Na_8. One observes a large internal excitation of the cluster while comparatively little perturbation goes to the substrate and there is again the clear distinction between deposition for lower impact energies and reflection for higher ones. But there are several interesting differences in detail. Most of all, there is a strong lateral drift in all cases. Indeed the pentagonal ring of Na_6 does not match the rectangular structure of MgO, which hinders it from fully accommodating the attractive oxygen sites. Thus, one or two corners of the pentagon are bent up during the deposition process, and this, in turn, induces a sizeable lateral momentum (see right panels of Fig. 6), and a strong perturbation of the pentagon, as can be deduced from the motion of z coordinates shown in the left panels. In the case of the robust deposition, the cluster even rolls over the surface. The stronger lateral excitation

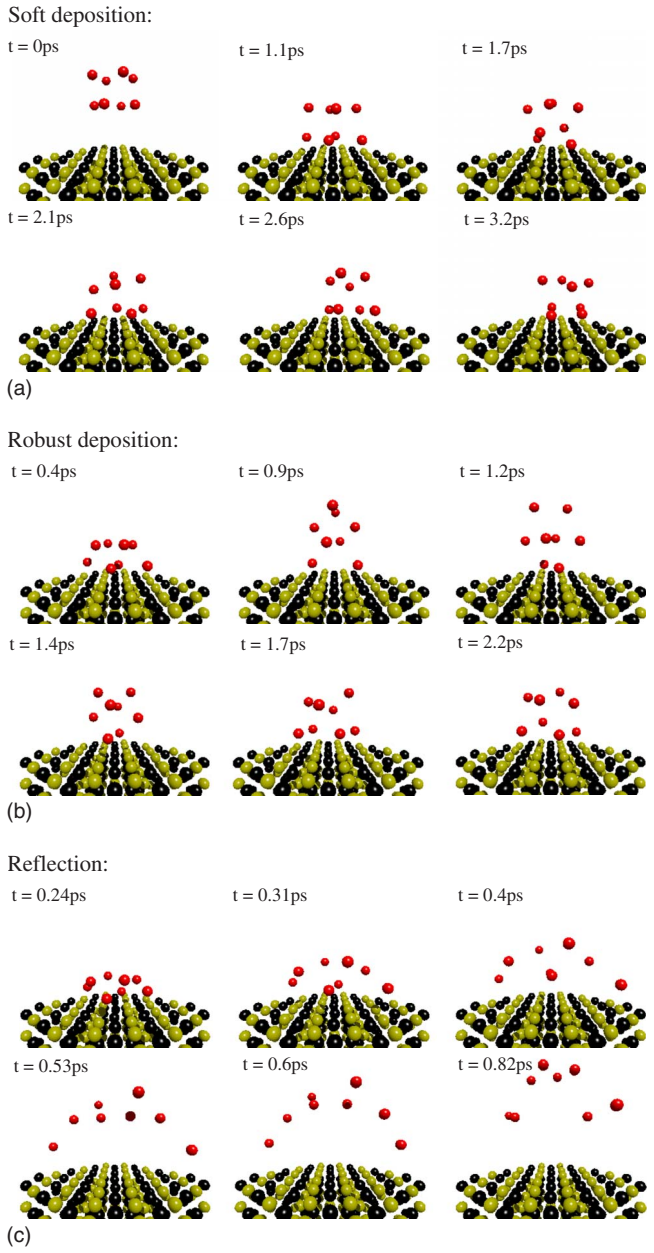

FIG. 5. (Color online) Snapshots of the time evolution for three cases of collisions of Na_8 on MgO(001) with different initial kinetic energies E_{kin}. Upper panel : Soft deposition with $E^0_{kin}=0.109$ eV. Middle panel : Robust deposition with $E^0_{kin}=1.09$ eV. Lower panel : Reflection with $E^0_{kin}=10.9$ eV.

leaves also somewhat more perturbation to the substrate than in the case of Na_8, as may be spotted when comparing Figs. 4 and 6. That will become more obvious when checking energies in Sec. III D. Finally, it is interesting to note that the cluster orientation is also reverted in the case of reflection. The z coordinates (upper left panel in Fig. 6) suggest a process where the ring and the former top ion are reflected "independently" such that the topping ion is departing "behind/after" the ring, and thus, reverting the cluster orientation.

As noted above, when deposited, the Na_6 experiences a sizable drift due to the mismatch of its structure with the crystalline structure of MgO. One, thus, expects that direction and strength of the lateral motion depend sensitively on the initial position and orientation of Na_6 relative to the surface. Indeed Fig. 7 shows the trajectory of the center-of-mass of the Na_6 cluster projected onto the x-y-plane for three different initial orientations. There are obviously dramatic differences. The cluster is kicked to a strong lateral motion for initial impact at repulsive sites (Mg, hollow) while only moderate lateral drift appears for impact on the attractive O site.

One can learn more about the electronic charge distribution in the cluster during a collision by a direct multipole analysis of this distribution. We discuss here briefly the lowest nontrivial moments, the dipoles. Figure 8 shows the time evolution of dipole polarization for two different scenarios, deposition vs. reflection. The figure is augmented by the time-evolution of the center-of-mass as global indicator of the dynamical situation (lower panels). The two scenarios differ by the initial kinetic energies, the lower value related to a more or less soft deposition, while the higher initial velocity leads to immediate reflection of the cluster, as discussed above. In the slow deposition process (left panels), there is a strong increase in the z polarization at the time of closest impact. This polarization remains during the further evolution at about 10% of the Wigner-Seitz radius, hence, represents a considerable internal polarization. Also, some x-y polarization builds up during the ongoing deposition oscillations. In contrast, in the case of a reflection (right panels), one sees a large instantaneous polarization at the time of closest approach, but only a very small remaining effect when the cluster has departed from the surface. The very short interaction time limits the internal excitation.

C. MgO versus Ar Substrate

In previous works,[33,47] the deposition of Na_6 on a cold, condensed argon substrate Ar(001) was investigated. Like MgO, solid Ar has a large band gap. But apart from this insulating nature, the two materials have much different properties. The attractive interaction between MgO and Na is much stronger than between Ar and Na, due to the larger polarizability of the oxygen ion. On the other hand, frozen Ar material is a very soft solid due to the weak Ar-Ar binding. The melting point of Ar is 83.78 K,[58] much lower than that of MgO around 3073 K.[59] The softness of the Ar material, thus, changes the energy balance to the extent that the Ar substrate takes up most of the impinging energy, leaving rather little internal excitation for the cluster itself. Thus Ar substrates are very efficient soft stopper materials. In the former analysis,[33,47] we had run a similar series of impact energies as above and we also found soft deposition for energies up to at least $E^0_{kin}/N_{ion}=0.272$ eV. An attempt to reach a reflection regime by further increasing the impact energy then led to a significant destruction of the substrate. Figure 9 illustrates that violent collision of Na_6 on an Ar(001) surface. The cluster is indeed finally reflected, but the process evolves much different from the case of the collision with MgO shown in Fig. 6. The cluster is not reflected instantaneously, as for MgO, but with a delay of about 500 fs. It requires an additional boost from momentum reflected by the

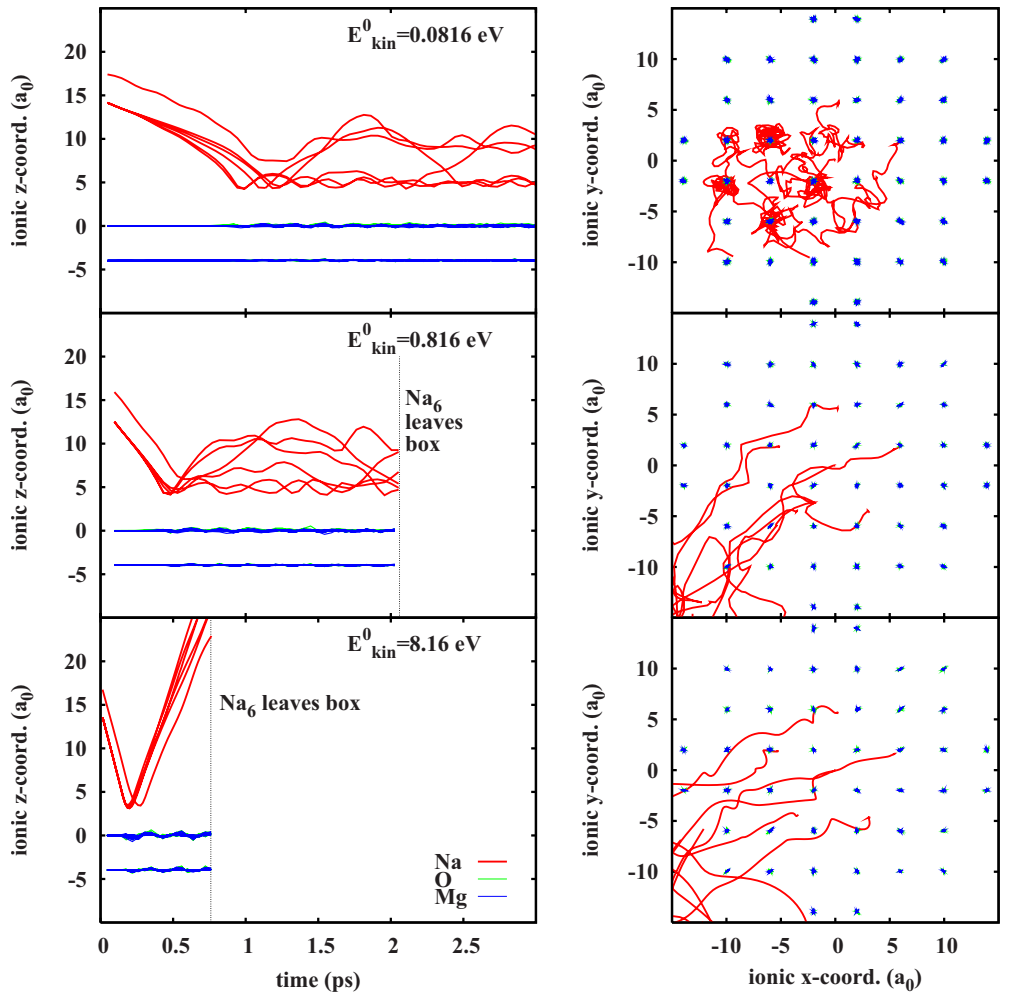

FIG. 6. (Color online) Left : Time evolution of the ionic z-coordinates of Na_6 approaching MgO(001). Right : Projection of the Na and MgO trajectories into the x-y-plane; the figures are vertically sorted by increasing initial kinetic energy : Soft deposition (top), robust deposition (center), reflection (top).

first Ar layer to finally release the cluster. Moreover, so much energy has been deposited in the weakly bound Ar material that the substrate is seriously damaged by that forced "reflection." These significant differences between Ar and MgO substrate will also be seen in the energy analysis later on.

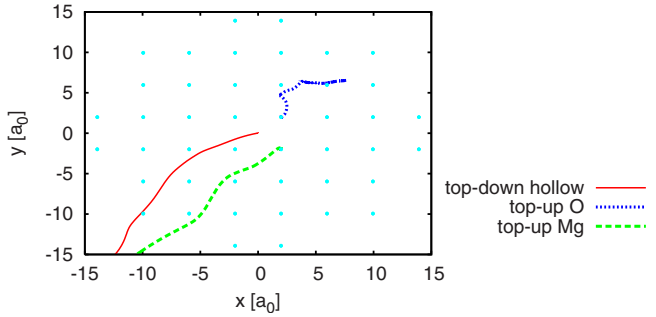

FIG. 7. (Color online) The trajectories of the Na_6 center of mass, projected on a plane parallel to the surface. The lateral drift sensitively depends on the site above which the cluster impinges (hollow, O or Mg site) and on its orientation (top ion above—up—and top ion below—down—the ring).

D. Energy Transfer

1. Time evolution of energy components

A complementing view of the deposition dynamics is given by the kinetic energies. Figure 10 shows the time evolution of the kinetic energies for Na and MgO. The kinetic energy for the Na cluster is furthermore splitted into center-of-mass energy and intrinsic kinetic energy (from the motion relative to the center-of-mass). Let us first consider the case of reflection (upper panel). In the approaching phase, the cluster is accelerated by about 0.68 eV, which is small compared to the initial energy 10.9 eV. Dramatic and fast changes emerge at impact time at 200 fs. The cluster kinetic energy exhibits a deep minimum. In that stage, almost all energy is stored in deformation. A large part of that deformation energy is quickly released showing up now as intrinsic kinetic energy of the cluster plus a smaller bit in translational energy. Another small fraction of energy is transferred to the substrate. The translational kinetic energy decreases further on, because the departing cluster has to work against the attractive polarization interaction. Still, there remains sufficient translational energy to allow the cluster to finally escape, as in a very inelastic collision.

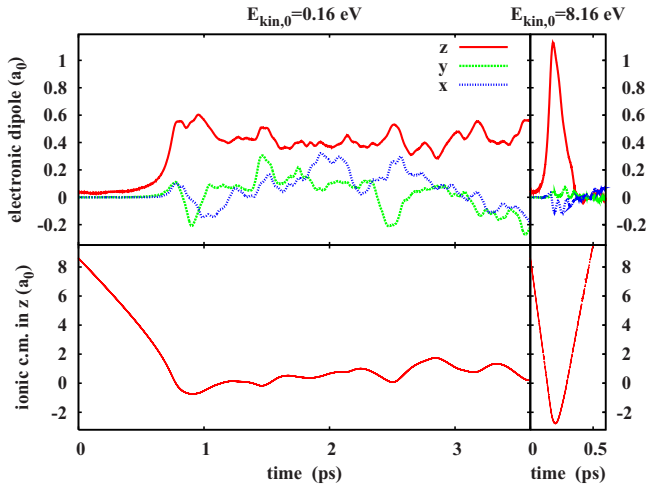

FIG. 8. (Color online) Dipole polarization of the cluster electrons during collision of Na_6 on MgO(001). Upper panels: Dipole moments of the electron cloud of the Na_6 cluster in x-y-(horizontal) and z-direction as function of time. Lower panels: Time-evolution of the z component of the center-of-mass of the Na_6 cluster; the line $z=0$ corresponds to the center of mass of a fully relaxed configuration of Na_6 on MgO(001). Left panels: case of soft deposition at rather low-initial kinetic energy (as indicated). Right panels: case of more energetic collision which leads to immediate reflection.

Similar results are found for the soft (lower panel in Fig. 10) and robust deposition (middle panel). Again, only a small fraction of the energy is transferred to the substrate, another small fraction goes to the cluster center-of-mass oscillations, and the major part to intrinsic energy of the cluster. Particularly interesting is the case of robust deposition (middle panel) where it requires a second bounce to stir up intrinsic cluster motion. Before that, there is still enough energy in translation to allow a lateral hopping from one attractive MgO site to the next (see also Fig. 4). It is worth noting that the average trend of the kinetic energy of MgO in Fig. 10 has a small, but nonvanishing, slope. The cluster continues to exchange energy with the substrate on a very slow pace. That indicates a thermalization process which eventually leads to equidistribution of kinetic energies after long time, however much beyond our simulation capabilities.

The present modeling includes an independent dynamics of the dipole moments of the oxygen anions in the substrate.

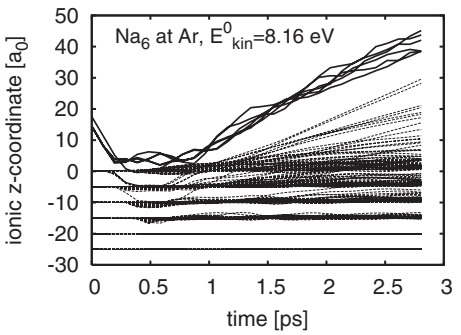

FIG. 9. Time evolution of z coordinates during collision of Na_6 with initial total kinetic energy $E^0_{kin}=8.16$ eV (1.36 eV per Na atom) on an Ar(001) surface. Data taken from.[47]

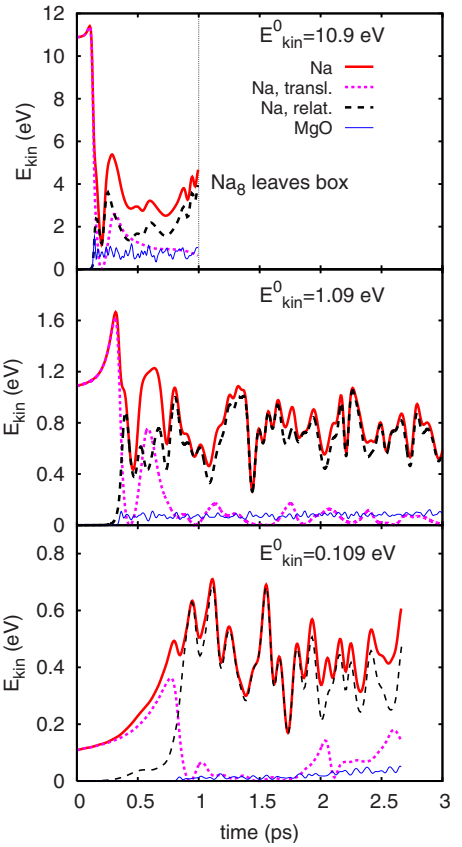

FIG. 10. (Color online) Time evolution of various contributions to kinetic energy for the collision of Na_8 with MgO(001) at three different initial kinetic energies as indicated. Contributions are : Total kinetic energy of the cluster ions (Na, thick curves), contributions due to center of mass motion (Na transl., dashes) and relative motion or heat (Na relat., dots), and total kinetic energy of the substrate (MgO, thin curves).

It has been shown recently that a significant amount of energy can be stored in these degrees-of-freedom when a metal cluster is deposited on an Ar surface.[35,36] One can define a dipole energy which scales as the square of the dipole amplitudes. Figure 11 shows a typical result for the time evolution of the energy contained in the oscillating dipoles in the case of reflection of Na_6 deposited on MgO. There is a small initial value which corresponds well to the finite initial dis-

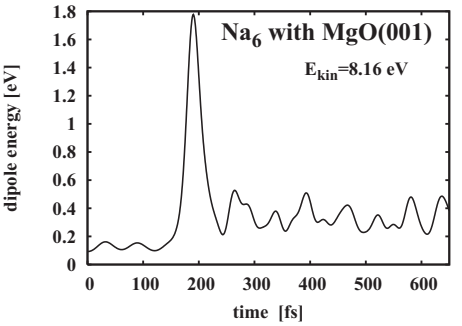

FIG. 11. Time evolution of the dipole polarization energy in the MgO(001) substrate for the collision for Na_6 with MgO(001) at an initial kinetic energy of 8.16 eV (reflection case).

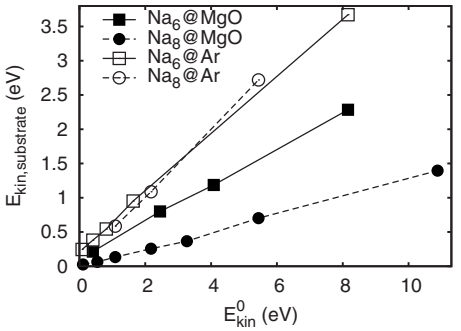

FIG. 12. Heating of the MgO or Ar substrate after impact of Na_6 and Na_8. The energy transfer to Ar is independent of the cluster structure, whereas the energy transfer to MgO is not. Na_6 transfers about twice as much energy as the compact Na_8.

tance of the Na cluster to the substrate. There is a large contribution at the time of closest impact. This part is dominated by (instantaneous) static polarization which would also be contained in a Born-Oppenheimer MD. The dipole energy falls back to lower values when the cluster departs from the substrate (see Fig. 6). But there remains some offset which corresponds to the energy finally transferred to the dipole degrees of freedom. It amounts to about 2% of the impact energy, which is small compared to the other energetic observables, see Fig. 14 and corresponding discussion in Sec. III. In contrast to the case of Ar substrate, energy transfer to MgO dipoles has actually only a small effect for the overall ionic dynamics. But more subtle properties as optical response and trajectories of free charges (to be discussed in a subsequent publication) will be sensitive to such details.

2. Energy transfers "at" impact

Notwithstanding asymptotic thermalization, the fast energy transfer to the substrate in the early stages is an interesting observable characterizing the collision process. Figure 12 shows the kinetic energy of the substrate soon after the collision, i.e. averaged over the first 2 ps after impact, as a function of the initial kinetic energy of the cluster E^0_{kin}. Apparently the energy absorbed by the substrate is proportional to E^0_{kin}. But the slope depends very much on cluster and surface types. The soft Ar substrate absorbs much more energy than MgO, typically a bit more than 50% of the initial kinetic energy. The softness and the rather small surface corrugation of Ar make the process insensitive to the actual cluster, which is approaching. That is different for MgO. There is always less energy absorption by the substrate and there is a strong dependence on the cluster configuration. Na_6 transfers more than twice as much energy as Na_8. The strong surface corrugation of MgO induces that sensitivity to cluster geometry. Remind that Na_6 does not match very well to the MgO surface while Na_8 does (see Sec. II F).

More information about what is happening directly around impact time can be obtained by reading off observables at shorter time scales (shorter than the 2 ps used above). Figure 13 shows two such observables as a function of initial kinetic energy. The upper panel shows the energy gain in the approaching phase due to the acceleration by the

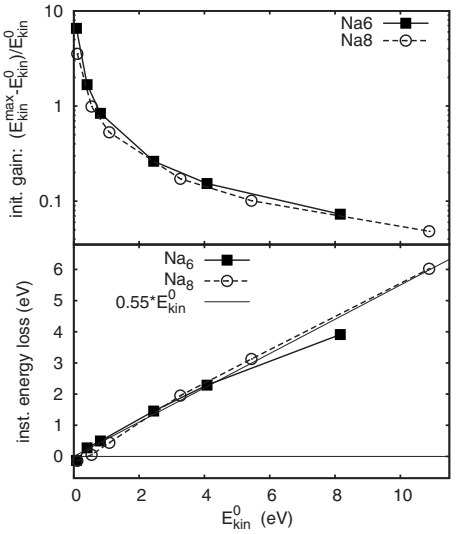

FIG. 13. Upper panel : The gain in kinetic energy of the cluster when approaching the MgO surface; lower panel : Instantaneous energy loss, defined as the difference between maximum kinetic energy before the impact and next maximum after impact.

polarization potential. It is defined as the difference of the first maximum of the cluster kinetic energy and the initial energy. Na_6 acquires slightly more energy than Na_8 because it has a nonvanishing dipole moment which, in turn, enhances the polarization attraction. There is a large gain in the low-energy range (the regime of soft deposit), while the trend becomes very flat for fast collisions. This is probably due to a move from adiabatic to nonadiabatic relaxation processes in the surface. For very low-impact velocities, the surface ions have time to follow the forces from the cluster, whereas for very high velocities the surfaces ions do not have enough time to respond before the cluster collides. The lower panel of figure 13 shows an attempt to quantify an "instantaneous energy loss." To that end, we take difference between the maximum kinetic energy before the impact and the next maximum after the impact. Obviously the instantaneous energy transfer is practically the same for Na_6 and Na_8 independent of their differences in structure; and the energy loss is approximately proportional to E^0_{kin}. About half (more precisely around 55%) of the impact energy is withdrawn from the cluster in that first round.

3. Redistribution of initial kinetic energy

It is, furthermore, interesting to see how the initially available energy is distributed over the various constituents. Such energy balance is shown in Fig. 14 as a function of E^0_{kin}. All energies have been averaged over 2 ps after impact time. They are drawn relative to the maximum kinetic energy of the cluster before impact. The energy terms do not necessarily sum up to one because the interaction between substrate and cluster is omitted, as well as the intrinsic potential energy of the cluster. Low energies (<2.72 eV for Na_8 and <2.18 eV for Na_6) represent the regime of deposition. The largest amount of energy is used up here for intrinsic cluster motion combined with potential energy of the substrate. The latter is responsible for the attachment of the cluster to the

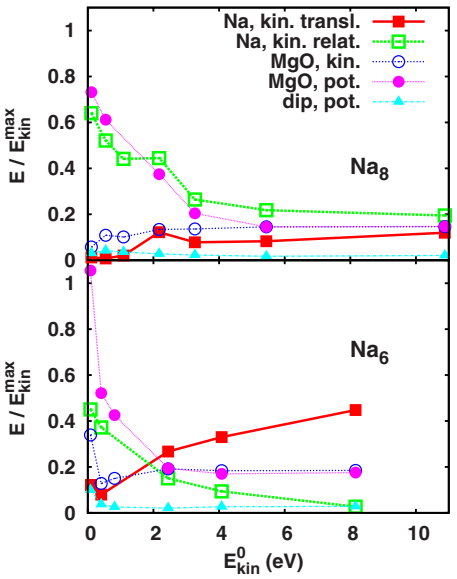

FIG. 14. (Color online) Distribution of impact energy amongst various components : Kinetic energy of the cluster (split into intrinsic, open squares, and translational, close squares, motion), kinetic energy of the MgO substrate (open circles), potential energy in the oxygen dipoles (triangles), and other potential energy in the substrate (close circles). Upper panel : Na_8 with MgO, lower panel : Na_6 with MgO.

surface. The higher energies represent the regime of reflection. The share of energies depends here on the cluster geometry. For Na_6, the translational motion takes the lead, whereas the intrinsic motion shrinks to almost zero. That complies with the trajectories in Fig. 6, which show that the cluster is repelled from the surface with opposite orientation but only weakly perturbed structure. The reflection of the top ion seems to proceed independently from the five-fold ring. The ring hits first and departs first while the top ion is reflected later, thus, departing behind the ring.

For both clusters, kinetic and potential energies of the MgO behave similar. For high E^0_{kin} in the reflection regime, potential and kinetic energy are equal. The cluster quickly transfers some momentum to the substrate at impact and then disappears. This leaves the substrate ions oscillating around their equilibrium positions in harmonic motion, associated to equipartition between kinetic and potential energy. For high E^0_{kin} in the soft landing domain, the situation is different. The potential energy becomes the dominant contribution because the cluster is adsorbed and remains in contact with the surface. This distorts the surface and leads to a large potential energy. Polarization energy is dominating in the potential energy. But the isolated contribution from the oxygen dipoles, also shown in Fig. 14, is comparatively small. The polarization within the oxygen ions in fact remains small as compared to the polarization caused by the displacement of O versus Mg, each one carrying a net charge of $\pm 2e$.

IV. CONCLUSIONS

We have analyzed the dynamics of deposition of small Na clusters on an MgO surface taking up a well tested hierarchical QM/MM modeling where the cluster electrons are treated quantum mechanically by time-dependent local-density approximation and the cluster ions as well as the substrate atoms by classical molecular mechanics. The dynamical polarizability of the substrate atoms is taken into account to describe correctly the strong polarization effects in the cluster–material interaction. The results are compared to deposition on Ar surface which is much softer than MgO.

Test cases were Na_6, which is a strongly oblate cluster with a finite dipole momentum, and the well bound and highly symmetrical Na_8. The general pattern are similar : The clusters are very quickly stopped by the substrate, they transfer a rather small amount of energy to the substrate while acquiring strong internal excitation. For larger impact energies, the clusters are reflected from the surface. This reflection is, of course, inelastic and leaves the clusters departing in highly excited intrinsic motion. There are, on the other hand, significant differences between the two cases, since the cluster geometry has a large influence on the dynamics. The main effects come from the strong surface corrugation of MgO(001). Na_6 does not match the surface structure and thus acquires significant lateral motion in contrast to Na_8, which keeps better on a vertical track. Moreover, Na_6 transfers more energy to the substrate than Na_8.

In comparison to Ar(001) surface, we find a similar energy range for deposition and reflection. The details, however, differ dramatically. Deposition on Ar(001) transfers most of the energy to the substrate leaving a rather mildly excited cluster on the surface while there is very little energy transfer to MgO(001) and large intrinsic excitation of the cluster. Reflection from Ar(001) is achieved at the price of severe surface destruction while MgO remains intact at the danger that the highly excited departing cluster may fragment later on.

The detailed energy balance differs in the deposition and reflection regime. In case of deposit, most energy is going to intrinsic cluster excitation and substrate polarization. In case of reflection, there is, of course, more translational energy left for the cluster and the substrate develops equipartition of kinetic and potential energy related to the remaining small, nearly harmonic, oscillations.

ACKNOWLEDGMENTS

This work was supported by the Deutsche Forschungsgemeinschaft (Grants No. RE 322/10-1 and No. RO 293/27-2), Fonds der Chemischen Industrie (Germany), a Bessel-Humboldt prize, and a Gay-Lussac prize.

[1] *Metal Clusters at Surfaces*, edited by K. H. Meiwes-Broer (Springer, Berlin, 2000).
[2] C. Binns, Surf. Sci. Rep. **44**, 1 (2001).
[3] Appl. Phys. A **82** (2006), special issue on *Clusters at Surfaces: Electronic Properties and Magnetism*, edited by K.-H. Meiwes-Broer.
[4] Eur. Phys. J. D **45** (2007), topical issue on *Atomic Clustes at Surfaces and in Thin Films*, edited by K.-H. Meiwes-Broer and R. Berndt.
[5] *Chemisorption and Reactivity of Supported Clusters and Thin Films*, edited by R. M. Lambert and G. Pacchioni, NATO Advanced Studies Institute, Series E: Applied Science (Kluwer, Dordrecht, 1997), Vol. 331.
[6] K. Watanabe, D. Menzel, N. Nilius, and H.-J. Freund, Chem. Rev. (Washington D.C.) **106**, 4301 (2006).
[7] N. Rösch, V. A. Nasluzov, K. M. Neyman, G. Pacchioni, and G. N. Vayssilov, in *Computational Material Science*, edited by J. Leszczynski, Theoretical and Computational Chemistry Series Vol. 15 (Elsevier, Amsterdam, 2004), p. 367.
[8] *Nanocatalysis*, edited by U. Heiz and U. Landman (Springer, Berlin, 2006).
[9] H.-J. Freund, M. Bäumer, and H. Kuhlenbeck, Adv. Catal. **45**, 333 (2000).
[10] A. Sanchez, S. Abbet, U. Heiz, W.-D. Schneider, H. Häkkinen, R. N. Barnett, and U. Landman, J. Phys. Chem. A **103**, 9573 (1999).
[11] T. Diederich, J. Tiggesbäumker, and K. H. Meiwes-Broer, J. Chem. Phys. **116**, 3263 (2002).
[12] A. Pinchuk, A. Hilger, G. von Plessen, and U. Kreibig, Nanotechnology **15**, 1890 (2004).
[13] F. Fehrer, P. M. Dinh, E. Suraud, and P.-G. Reinhard, Phys. Rev. B **75**, 235418 (2007).
[14] Y. Z. Li, R. Reifenberger, and R. P. Andres, Surf. Sci. **250**, 1 (1991).
[15] D. M. Schaefer, A. Patil, R. P. Andres, and R. Reifenberger, Phys. Rev. B **51**, 5322 (1995).
[16] C. Kuhrt and M. Harsdorff, Surf. Sci. **245**, 173 (1991).
[17] K. Bromann, C. Félix, H. Brune, W. Harbich, R. Monot, J. Buttet, and K. Kern, Science **274**, 956 (1996).
[18] S. Fedrigo, W. Harbich, and J. Buttet, Phys. Rev. B **58**, 7428 (1998).
[19] J. T. Lau, W. Wurth, H.-U. Ehrke, and A. Achleitner, Low Temp. Phys. **29**, 223 (2003).
[20] C. Sieber, W. Harbich, K.-H. Meiwes-Broer, and C. Félix, Chem. Phys. Lett. **433**, 32 (2006).
[21] S. Duffe, T. Irawan, M. Bieletzki, T. Richter, B. Sieben, C. Yin, B. V. Issendorff, M. Moseler, and H. Hövel, Eur. Phys. J. D **45**, 401 (2007).
[22] C. Xirouchaki and R. E. Palmer, Vacuum **66**, 167 (2002).
[23] H. P. Cheng and U. Landmann, Science **260**, 1304 (1993).
[24] H. Haberland, Z. Insepov, and M. Moseler, Z. Phys. D **26**, 229 (1993).
[25] R. P. Webb, Radiat. Eff. Defects Solids **162**, 567 (2007).
[26] T. T. Järvi, A. Kuronen, K. Meinander, K. Nordlund, and K. Albe, Phys. Rev. B **75**, 115422 (2007).
[27] H. Häkkinen and M. Manninen, Europhys. Lett. **34**, 177 (1996).
[28] H. Häkkinen and M. Manninen, J. Chem. Phys. **105**, 10565 (1996).
[29] M. Moseler, H. Häkkinen, and U. Landman, Phys. Rev. Lett. **89**, 176103 (2002).
[30] A. Ipatov, E. Suraud, and P. G. Reinhard, Int. J. Mol. Sci. **4**, 301 (2003).
[31] A. Ipatov, P.-G. Reinhard, and E. Suraud, Eur. Phys. J. D **30**, 65 (2004).
[32] C. Inntam, L. V. Moskaleva, K. M. Neyman, V. A. Nasluzov, and N. Rösch, Appl. Phys. A: Mater. Sci. Process. **82**, 181 (2006).
[33] P. M. Dinh, F. Fehrer, P.-G. Reinhard, and E. Suraud, Eur. Phys. J. D **45**, 415 (2007).
[34] P. Jensen, Rev. Mod. Phys. **71**, 1695 (1999).
[35] P. M. Dinh, F. Fehrer, P.-G. Reinhard, and E. Suraud, Surf. Sci. **602**, 2699 (2008).
[36] P. M. Dinh, P.-G. Reinhard, and E. Suraud, Surf. Sci. **603**, 400 (2009).
[37] M. Bär, L. V. Moskaleva, M. Winkler, P.-G. Reinhard, N. Rösch, and E. Suraud, Eur. Phys. J. D **45**, 507 (2007).
[38] W. A. de Heer, Rev. Mod. Phys. **65**, 611 (1993).
[39] M. Brack, Rev. Mod. Phys. **65**, 677 (1993).
[40] S. Bjornholm and J. Borggreen, Philos. Mag. **79**, 1321 (1999).
[41] M. J. Field, P. A. Bash, and M. Karplus, J. Comput. Chem. **11**, 700 (1990).
[42] J. Gao, Acc. Chem. Res. **29**, 298 (1996).
[43] N. Gresh and D. R. Garmer, J. Comput. Chem. **17**, 1481 (1996).
[44] P. J. Mitchell and D. Fincham, J. Phys.: Condens. Matter **5**, 1031 (1993).
[45] V. A. Nasluzov, K. Neyman, U. Birkenheuer, and N. Rösch, J. Chem. Phys. **115**, 8157 (2001).
[46] B. Gervais, E. Giglio, E. Jaquet, A. Ipatov, P.-G. Reinhard, and E. Suraud, J. Chem. Phys. **121**, 8466 (2004).
[47] F. Fehrer, Ph.D. thesis, Universität Erlangen/Nürnberg, 2006.
[48] F. Fehrer, M. Mundt, P.-G. Reinhard, and E. Suraud, Ann. Phys. (Leipzig) **14**, 411 (2005).
[49] F. Calvayrac, P.-G. Reinhard, E. Suraud, and C. A. Ullrich, Phys. Rep. **337**, 493 (2000).
[50] P.-G. Reinhard and E. Suraud, *Introduction to Cluster Dynamics* (Wiley, New York, 2003).
[51] B. G. Dick and A. W. Overhauser, Phys. Rev. **112**, 90 (1958).
[52] C. Legrand, E. Suraud, and P.-G. Reinhard, J. Phys. B **35**, 1115 (2002).
[53] M. Winkler, diploma thesis, Technische Universität München, 2006.
[54] F. Fehrer, P.-G. Reinhard, E. Suraud, E. Giglio, B. Gervais, and A. Ipatov, Appl. Phys. A: Mater. Sci. Process. **82**, 151 (2006).
[55] F. Fehrer, P.-G. Reinhard, and E. Suraud, Appl. Phys. A: Mater. Sci. Process. **82**, 145 (2006).
[56] V. Blum, G. Lauritsch, J. A. Maruhn, and P.-G. Reinhard, J. Comput. Phys. **100**, 364 (1992).
[57] M. D. Feit, J. A. Fleck, and A. Steiger, J. Comput. Phys. **47**, 412 (1982).
[58] J. Ancsin and M. J. Phillips, Metrologia **5**, 77 (1969).
[59] J. S. McDowell and R. M. Howe, J. Am. Ceram. Soc. **3**, 185 (1920).